Cobalt(II) Phenoxy-imine Complexes in Radical Polymerization of Vinyl acetate: The Interplay of Catalytic Chain Transfer and Controlled/Living Radical Polymerization

Yi-Hao Chen,[1†] Shih-Ji Chen,[1†] Jia-Qi Li,[1] Zhenqiang Wu,[2] Gene-Hsiang Lee,[3] Yi-Hung Liu,[3] Wei-Ting Cheng,[4] Chen-Yu Yeh,[4] Chi-How Peng[1]

[1]Department of Chemistry and Frontier Research Center on Fundamental and Applied Sciences of Matters, National Tsing Hua University, Hsinchu 30013, Taiwan
[2]Beijing National Laboratory for Molecular Sciences, State Key Lab of Rare Earth Materials Chemistry and Applications, College of Chemistry and Molecular Engineering, Peking University, Beijing 100871, China
[3]Instrumentation Center, National Taiwan University, Taipei 10617, Taiwan
[4]Department of Chemistry and Research Center for Sustainable Energy and Nanotechnology, National Chung Hsing University, Taichung 402, Taiwan
Correspondence to: C.-H. Peng (E-mail: chpeng@mx.nthu.edu.tw)

Received 20 June 2019; Revised 29 July 2019; accepted 31 July 2019
DOI: 10.1002/pola.29460

ABSTRACT: A series of cobalt(II) phenoxy-imine complexes ($Co^{II}(FI)_2$) have been synthesized to mediate the radical polymerization of vinyl acetate (VAc) and methyl acrylate (MA) to evaluate the influence of chelating atoms and configuration to the control of polymerization. The VAc polymerizations showed the properties of controlled/living radical polymerization (C/LRP) with complexes **1a** and **3a**, but the catalytic chain transfer (CCT) behaviors with complexes **2a**, **1b**, **2b**, and **3b**. The control of VAc polymerization mediated by complex **1a** could be improved by decreasing the reaction temperature to approach the molecular weights that not only linearly increased with conversions but also matched the theoretical values and relatively narrow molecular weight distributions. The catalytic chain transfer polymerizations (CCTP) mediated by complexes **2a**, **1b**, **2b**, and **3b** were characterized by Mayo plots and the polymer chain end double bonds were observed by ^{1}H NMR spectra. The tendency toward C/LRP or CCTP in VAc polymerization mediated by $Co^{II}(FI)_2$ could be determined by the ligand structure. Cobalt complex coordinated by the ligand with more steric hindered and less electron-donating substituents favored the controlled/living radical polymerization. In contrast, the efficiency of CCT process could be enhanced by less steric hindered, more electron-donating ligands. The controlled/living radical polymerization of MA, however, could not be achieved by the mediation of these cobalt(II) phenoxy-imine complexes. Associated with the results of polymerization mediated by other cobalt complexes, this study implied that the configuration and spin state of cobalt complexes were more critical than the chelating atoms to the control behavior of radical polymerization. © 2019 Wiley Periodicals, Inc. J. Polym. Sci., Part A: Polym. Chem. **2019**

KEYWORDS: catalytic chain transfer; cobalt; controlled/living radical polymerization; Phenoxy-imine; Vinyl acetate

INTRODUCTION Cobalt complexes have played an important role in the radical polymerization of vinyl monomers. Since 1975, cobalt porphyrin complex has been applied to accelerate the chain transfer reaction in methyl methacrylate polymerization, which was reported by Smirnov et al. and Gridnev.[1–3] The cobaloxime [$Co^{II}(dmgH)_2$, Scheme 1(a)] was then found to be a highly efficient catalytic chain transfer (CCT) agent in methyl methacrylate radical polymerization[4–10] and was industrialized for the preparation of polymeric products with low-molecular weight.[11,12] Recently, Engelis et al. used the cobaloxime to synthesize the sequential-controlled multiblock copolymers.[13] Poli et al. expanded this area by developing a new cobalt complex, $Co^{II}(OPN)_2$ [Scheme 1(b)], to mediate the catalytic chain transfer polymerization (CCTP) of vinyl acetate (VAc).[14] More details of recent progress in CCTP could be found in the review article published by Heuts and Smeets.[15]

In addition to catalytic CCTP, cobalt complexes have also shown a remarkable capability to achieve the controlled/living radical polymerization (C/LRP) of both conjugated vinyl monomers and

Additional supporting information may be found in the online version of this article.

†These authors contributed equally to this work.

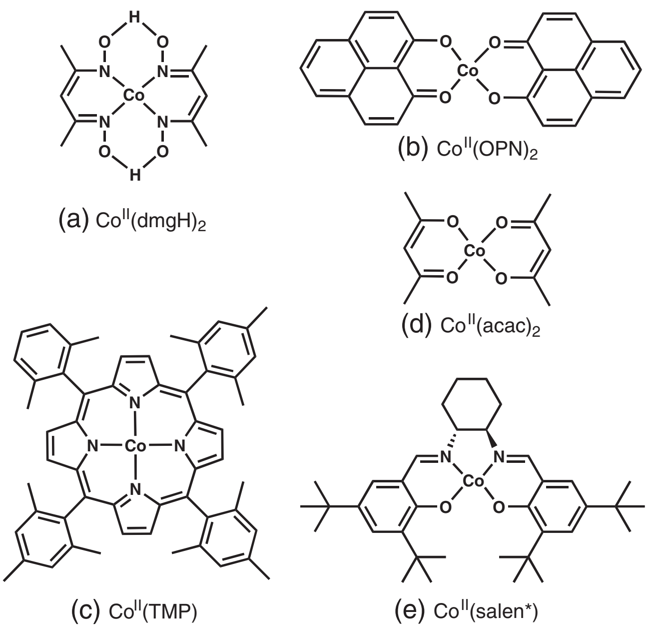

(a) $\mathrm{Co^{II}(dmgH)_2}$ (b) $\mathrm{Co^{II}(OPN)_2}$ (c) $\mathrm{Co^{II}(TMP)}$ (d) $\mathrm{Co^{II}(acac)_2}$ (e) $\mathrm{Co^{II}(salen^*)}$

SCHEME 1 Examples of cobalt complexes used to mediate radical polymerization. (a) $\mathrm{Co^{II}(dmgH)_2}$ (cobaloxime); (b) $\mathrm{Co^{II}(OPN)_2}$ (cobalt(II) 9-oxyphenalenone); (c) $\mathrm{Co^{II}(TMP)}$ (cobalt (II) tetramesitylporphyrin); (d) $\mathrm{Co^{II}(acac)_2}$ (cobalt (II) acetylacetonate); (e) $\mathrm{Co^{II}(salen^*)}$ (cobalt(II) [*N,N*′-bis(3,5-di-*tert*-butylsalicylidene)-1,2-cyclohexanediamine]).

unconjugated vinyl monomers.[16–23] Cobalt(II) porphyrin complex, $\mathrm{Co^{II}(TMP)}$ [Scheme 1(c)], was first reported to mediate the controlled/living radical polymerization (C/LRP) of methyl acrylate (MA) by Wayland et al.[24] Another milestone was attributed to Jérôme et al. who used cobalt(II) acetylacetonate [$\mathrm{Co^{II}(acac)_2}$, Scheme 1(d)] to control the VAc polymerization.[25] Afterward, several cobalt complexes were then applied to mediate controlled/living radical polymerization.[26–29] However, the ligand effect has not been systematically studied. Particularly, the comparison of $\mathrm{Co^{II}(TMP)}$ and $\mathrm{Co^{II}(acac)_2}$ is one of interest to polymer scientists because they have totally different coordinating atoms, configuration, and spin state. Although the use of $\mathrm{Co^{II}(salen^*)}$, a cobalt complex with square planar O,N,N,O-coordinated environment [Scheme 1(e)], as a mediator in C/LRP[30–33] provided a reference between $\mathrm{Co^{II}(TMP)}$ and $\mathrm{Co^{II}(acac)_2}$ from the aspect of coordinating atoms, the influence of configuration, and spin state of the cobalt complexes to the C/LRP is still ambiguous.

Herein, a series of cobalt(II) phenoxy-imine complexes ($\mathrm{Co^{II}(FI)_2}$, Scheme 2), which have same chelating atoms with $\mathrm{Co^{II}(salen^*)}$, but identical configuration and spin state with $\mathrm{Co^{II}(acac)_2}$, were selected to mediate the radical polymerization of VAc and MA for the investigation of ligand effect. The comparison of C/LRPs mediated by $\mathrm{Co^{II}(TMP)}$, $\mathrm{Co^{II}(salen^*)}$, $\mathrm{Co^{II}(FI)_2}$, and $\mathrm{Co^{II}(acac)_2}$ revealed that all four kinds of cobalt complexes can control the radical polymerization of VAc but only the cobalt complexes with low spin, square planar configuration can control the MA polymerization. Besides, cobalt(II) phenoxy-imine complexes were able to mediate the radical polymerization of VAc via C/LRP or CCTP pathway depending on the ligand structure. Controlled/living radical polymerization could be achieved by using cobalt complexes with more steric hindered and less electron-donating ligands. On the other hand, CCTP would be observed when the cobalt mediators had less steric hindered and more electron-donating ligands.

EXPERIMENTAL SECTION

Material

2,4-Di-*tert*-butylphenol (Alfa Aesar Ward Hill, Massachusetts, MA, USA), 2-hydrxoy-5-methoxybenzaldehyde (Lancaster), 3-*tert*-butyl-4-hydroxyanisole (Acros), VAc (Merck, 99%) were degassed by freeze-pump-thaw cycle for three times before use. Tributylamine (Alfa Aesar, 98%), tin(IV) chloride (Aldrich, 1.0 M in heptane), paraformaldehyde (Alfa Aesar, 97%), cyclohexylamine (Alfa Aesar, 98 + %), cobalt(II) acetate tetrahydrate (Acros, 97%), sodium hydroxide (SHIMAKYU'S), diphenyl(2,4,6-trimethyl-benzoyl)phosphine oxide (TPO, TCI, 98%), 2,2′-azobisisobutyronitrile (AIBN, Showa) were used without any purification. Toluene was dried by $\mathrm{CaH_2}$ before use.

Instruments

All manipulations were carried out under a dry nitrogen atmosphere using an MBraun glove box and Schlenk flask. NMR spectra were recorded by Mercury 400 MHz and 500 MHz Spectrometer. ^{1}H NMR chemical shifts are given in ppm versus residual protons in deuterated solvents as follows: δ 7.24 ppm ($\mathrm{CDCl_3}$). ^{13}C NMR chemical shifts are given in ppm versus residual ^{13}C in solvents as follows: δ 77 ppm ($\mathrm{CDCl_3}$). NMR spectroscopy was used to identify the ligand structure and monomer conversion. The UV–vis spectroscopy was measured by a SHIMADZU UV-1800 instrument from 1100 to 190 nm. The cyclic voltammetry (CV) was measured by three electrode potentiostat (CH Instruments, Model 750A) in $\mathrm{TBAPF_6/CH_2Cl_2}$ (0.1 M) using a Pt wire as the working electrode. The potentials were measured under scan rate = 0.1 V $\mathrm{s^{-1}}$ at 298 K with ferrocene as an internal standard. Polymers were characterized by a gel permeation chromatography (GPC) system equipped with three Shodex columns (Shodex KF-802, Shodex KF-803, and Shodex KF-805) using THF eluent at 30 °C and at a flow rate of 1.0 mL $\mathrm{min^{-1}}$. The signal was collected by DIONEX Shodex RI-101 refractometer (RI) detector. The molecular weight was calibrated with narrow linear poly(styrene) Shodex standard (SM-105) ranging in molecular weight from 1.20×10^{2} g $\mathrm{mol^{-1}}$–2.61×10^{6} g $\mathrm{mol^{-1}}$. Molecular weights and the M_w/M_n values were calculated using the DIONEX chromeleon software.

General Procedure for Polymerization of VAc and MA

$\mathrm{Co^{II}(FI)_2}$ (0.07 mmol) and AIBN (0.127 g, 0.77 mmol) were mixed in a 50 mL Schlenk flask and degassed by three vacuum/nitrogen cycles. Degassed VAc (5 mL, 54.24 mmol) was then injected into the Schlenk flask. The red mixture was heated to 60 °C under stir. The monomer conversion was measured by ^{1}H NMR. Molecular weight of polymer was measured by GPC. The polymerization of VAc at difference temperature and MA polymerization were performed under the same procedure.

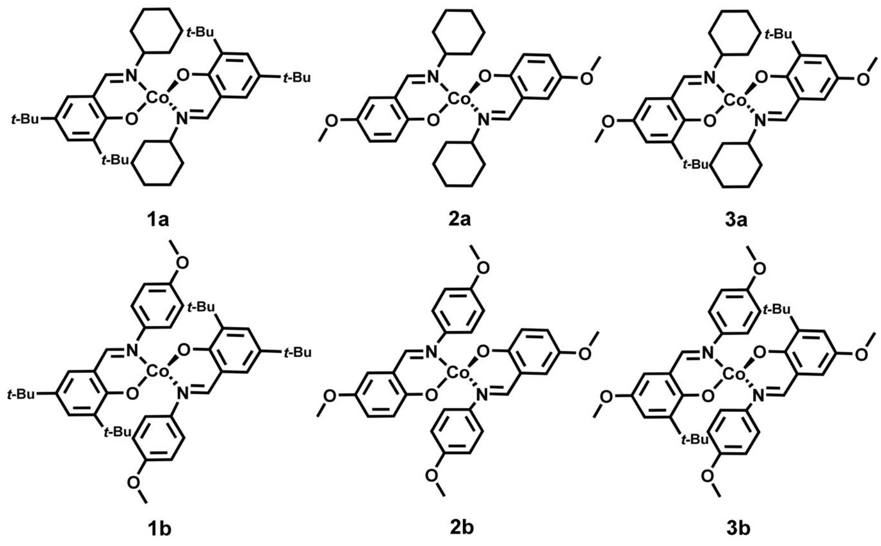

SCHEME 2 Structures of cobalt(II) phenoxy-imine complexes investigated in this study.

Photopolymerization of VAc

Photopolymerizations were carried out in a black box. The length, width, and height of the box were 26, 26, and 35 cm, respectively. Four UV lamps (PHILIPS, TL, 8 W, BLB, Poland) were used as the 365 nm light source. The sample was placed at an approximate distance of 12 cm to the lamps.

Chain Extension of VAc Polymerization Using Macro-Initiator Co-PVAc

Using a produce similar to general VAc polymerization. $(FI^{1a})_2Co^{III}$-PVAc was synthesized under the condition of $[\mathbf{1a}]_0/[TPO]_0/[VAc]_0$ = 1/5/500 at 24 °C in bulk by light initiated polymerization. After the desired conversion was obtained, residual VAc was removed under vacuum. Then, fresh VAc was added into the mixture, and chain extension of VAc polymerization was performed at 24 °C under UV light.

General Procedure for Preparing PVAc Macro-Monomer

PVAc macro-monomer was prepared with $Co^{II}(FI)_2$ as mediator under the condition of $[Co^{II}]_0/[AIBN]_0/[VAc]_0$ = 1/10/700 at 60 °C in bulk. The reaction was stopped by removing residual VAc under vacuum.

Synthesis of Aldehydes 1 and 3

Aldehydes were synthesized following the modified method based on literature.[34] Phenol (0.05 mol) and tributylamine (5 mL, 0.02 mol) were mixed with toluene (15 mL) in a 50 mL Schlenk flask under nitrogen. Tin(IV) chloride (1.0 M in heptane) was added to the solution dropwise under nitrogen atmosphere then the mixture reacted at room temperature for 15 min. Then, paraformaldehyde (2.078 g, 66.5 mmol) was added into solution and the solution was heated to 100 °C for another 10 h. The reaction was stopped by the addition of 100 ml water. The desired compound was then extracted by diethyl ether (30 mL) from the solution. The organic phase was separated, washed by water (200 mL), and dried over $MgSO_4$ before evaporation under reduced pressure. The crude product was purified by column chromatography (silica gel, hexane/EtOAc = 9/1). Yield of aldehyde **1** (3,5-di-*tert*-butyl-2-hdroxybenzaldehyde) was 75.3%, yellow solid. ^1H NMR (400 MHz, $CDCl_3$): δ (ppm) 11.62 (s, 1H, —O*H*), 9.85 (s, 1H, —C*H*O), 7.57 (d, *J* = 1.14 Hz, 1H, Ar-*H*), 7.33 (d, *J* = 1.24 Hz, 1H, Ar-*H*), 1.42 (s, 9H, $—C(CH_3)_3$), 1.31 (s, 9H, $—C(CH_3)_3$). ^{13}C NMR (100 MHz, $CDCl_3$): δ (ppm) 197.00, 158.86, 141.42, 137.39, 131.69, 127.67, 119.86, 35.09, 34.32, 31.41, 29.37. Yield of aldehyde **3** (3-(*tert*-butyl)-2-hdroxy-5-methoxybenzaldehyde) was 57.1%, yellow solid. ^1H NMR (400 MHz, $CDCl_3$): δ (ppm) 11.51 (s, 1H, —O*H*), 9.79 (s, 1H, -C*H*O), 7.15 (d, *J* = 1.54 Hz, 1H, Ar-*H*), 6.78 (d, *J* = 1.54 Hz, 1H, Ar-*H*), 3.78 (s, 3H, $—OCH_3$), 1.39 (s, 9H, $—C(CH_3)_3$). ^{13}C NMR (100 MHz, $CDCl_3$): δ (ppm) 196.20, 155.80, 151.72, 139.76, 123.58, 119.58, 111.48, 55.56, 34.93, 29.09.

Synthesis of Phenoxy-Imine (1a-3b)

Phenoxy-imine compounds were synthesized following the modified method based on literature.[34] Aldehyde (4.2 mmol) and amine (4.2 mmol) was dissolved in methanol (10.0 mL) and refluxed for 6 h under nitrogen atmosphere. The mixture was cooled to room temperature and the precipitation of yellow solid was observed. The product was filtrated and washed by cold methanol for three times and then dried under high vacuum. Yield of phenoxy-imine **1a** ((*E*)-2,4-di-*tert*-butyl-6-((cyclohexylimino)methyl)phenol) was 70.3%, yellow solid. ^1H NMR (400 MHz, $CDCl_3$): δ (ppm) 8.37 (s, 1H, —*H*C=N), 7.36 (s, 1H, Ar-*H*), 7.12 (s, 1H, Ar-*H*,), 3.14–3.24 (m, 1H, —C=NC*H*), 1.79 (d, *J* = 4.7 Hz, 4H, Cy-*H*), 1.50–1.65 (m, 6H, Cy-*H*), 1.42 (s, 9H, $—C(CH_3)_3$), 1.28 (s, 9H, $—C(CH_3)_3$). ^{13}C NMR (100 MHz, $CDCl_3$): δ (ppm) 163.25, 158.24, 139.76, 136.60, 126.51, 125.63, 117.96, 67.63, 35.01, 34.42, 34.09, 31.51, 29.45, 25.59, 24.48. Yield of phenoxy-imine **2a** ((*E*)-2-((cyclohexylimino) methyl)-4-methoxyphenol) was 62.4%, yellow solid. ^1H NMR (400 MHz, $CDCl_3$): δ (ppm) 8.30 (s, 1H, —*H*C=N), 6.85–6.90

(m, 2H, Ar-*H*), 6.74 (dd, *J* = 1.2, 0.4 Hz, 1H, Ar-*H*), 3.75 (s, 3H, —OCH_3), 3.16–3.25 (m, 1H, —C=NC*H*), 1.79 (d, *J* = 4.6 Hz, 4H, —Cy—*H*), 1.25–1.65 (m, 6H, —Cy—*H*). ^{13}C NMR (100 MHz, CDCl$_3$): δ (ppm) 161.62, 155.13, 151.60, 118.67, 118.43, 117.47, 114.56, 67.64, 55.93, 55.91, 34.34, 25.58, 24.41. Yield of phenoxy-imine **3a** ((*E*)-2-(*tert*-butyl)-6-((cyclohexylimino) methyl)-4-methoxyphenol) was 89.5%, yellow solid. ^{1}H NMR (400 MHz, CDCl$_3$): δ (ppm) 8.31 (s, 1H, —*H*C=N), 6.94 (d, *J* = 1.5 Hz, 1H, Ar-*H*), 6.59 (d, *J* = 1.4 Hz, 1H, Ar-*H*), 3.75 (s, 3H, —OCH_3), 3.15–3.24 (m, 1H, —C=NC*H*), 1.50–1.90 (m, 10H, —Cy—*H*), 1.41 (s, 9H, —C(CH_3)$_3$). ^{13}C NMR (100 MHz, CDCl$_3$): δ (ppm) 162.46, 154.80, 150.82, 138.70, 117.95, 117.61, 111.24, 67.74, 55.82, 55.81, 35.03, 34.47, 29.36, 25.65, 24.57. Yield of phenoxy-imine **1b** ((*E*)-2,4-di-*tert*-butyl-6-((phenylimino) methyl)phenol) was 87.3%, yellow solid. ^{1}H NMR (400 MHz, CDCl$_3$): δ (ppm) 8.65 (s, 1H, —*H*C=N), 7.42 (d, *J* = 1.2 Hz, 1H, Ar-*H*), 7.25–7.35 (m, 3H, Ar-*H*), 6.89 (d, *J* = 4.3 Hz, 1H, Ar-*H*), 3.81 (s, 3H, —OCH_3), 1.45 (s, 9H, —C(CH_3)$_3$), 1.30 (s, 9H, —C (CH_3)$_3$). ^{13}C NMR (100 MHz, CDCl$_3$): δ (ppm) 161.44, 158.29, 157.82, 141.41, 140.23, 136.63, 127.35, 126.39, 122.06, 118.30, 114.39, 55.48, 35.16, 34.25, 31.59, 29.54. Yield of phenoxy-imine **2b** ((*E*)-2-((cyclohexylimino)methyl)-4-methoxyphenol) was 90.3%, yellow solid. ^{1}H NMR (400 MHz, CDCl$_3$): δ (ppm) 8.56 (s, 1H, —*H*C=N), 7.24–7.30 (m, 2H, Ar-*H*), 6.95 (d, *J* = 0.8 Hz, 2H, Ar-*H*), 6.90–6.95 (m, 2H, Ar-*H*,), 6.89 (s, 1H, Ar-*H*), 3.83 (s, 3H, —OCH_3), 3.79 (s, 3H, —OCH_3). ^{13}C NMR (100 MHz, CDCl$_3$): δ (ppm) 159.74, 158.53, 154.87, 151.90, 141.04, 122.09, 119.61, 118.79, 117.66, 114.95, 114.37, 55.83, 55.44. Yield of phenoxy-imine **3b** ((*E*)-2-(*tert*-butyl)-4-methoxy-6-((phenylimino)methyl)phenol) was 63.5%, orange solid. ^{1}H NMR (400 MHz, CDCl$_3$): δ (ppm) 8.57 (s, 1H, —*H*C=N), 7.27 (d, *J* = 4.4 Hz, 2H, Ar-*H*), 7.00 (d, *J* = 1.6 Hz, 1H, Ar-*H*), 6.92 (d, *J* = 4.4 Hz, 2H, Ar-*H*), 6.72 (s, 1H, Ar-*H*), 3.82 (s, 3H, -OCH_3), 3.79 (s, 3H, —OCH_3), 1.44 (s, 9H, —C(CH_3)$_3$). ^{13}C NMR (100 MHz, CDCl$_3$): δ (ppm) 160.65, 158.41, 154.68, 151.17, 141.13, 138.95, 122.07, 118.68, 118.36, 114.40, 111.61, 55.75, 55.47, 35.08, 29.33.

Synthesis of Cobalt(II) Phenoxy-Imine Complexes

Cobalt(II) phenoxy-imine complexes were synthesized following the modified method based on the literature.[35] Phenoxy-imine (1.9 mmol), NaOH (0.9 mmol), and methanol (10 mL), which were mixed in a 50 mL Schlenk flask. Then cobalt(II) acetate (1.1 mmol) in MeOH solution was added dropwise to the mixture at 40 °C. The solution was subsequently heated to 60 °C and reacted for 6 h. The precipitate was filtered and washed by methanol (10 mL) for three times, and then dried under high vacuum to obtain Co^{II}(FI)$_2$ complexes. Yield of complex **1a** was 92.8%, yellow solid. Observed value in mass spectrum (FAB, *m*/*z*) was 687, matched well with calc. exact mass $C_{42}H_{64}CoN_2O_2$ 687.92. Anal. Calc. (found) for $C_{42}H_{64}CoN_2O_2$: N 4.07 (4.09), C 73.33 (73.08), H 9.38 (9.42) %. The maximum absorption wavelength and molar absorption coefficient were $\varepsilon_{300\ \text{nm}}$ = 11,000 L cm^{-1} mol^{-1}, $\varepsilon_{375\ \text{nm}}$ = 10,100 L cm^{-1} mol^{-1}. Yield of complex **2a** was 62.4%, red solid. Observed value in mass spectrum (FAB, *m/z*) was 524, matched well with calc. exact mass $C_{28}H_{36}CoN_2O_4$ 523.54. Anal. Calc. (found) for $C_{28}H_{36}CoN_2O_4$: N 5.35 (5.35), C 64.24 (64.30), H 6.93 (6.99) %. The maximum absorption wavelength and molar absorption coefficient were $\varepsilon_{307\ \text{nm}}$ = 7300 L cm^{-1} mol^{-1}, $\varepsilon_{395\ \text{nm}}$ = 8700 L cm^{-1} mol^{-1}. Yield of complex **3a** was 89.5%, orange solid. Observed value in mass spectrum (FAB, *m/z*) was 635, matched well with calc. exact mass $C_{36}H_{52}CoN_2O_4$ 635.76. Anal. Calc. (found) for $C_{36}H_{52}CoN_2O_4$: N 4.41 (4.43), C 68.01 (68.17), H 8.24 (8.38) %. The maximum absorption wavelength and molar absorption coefficient were $\varepsilon_{308\ \text{nm}}$ = 8200 L cm^{-1} mol^{-1}, $\varepsilon_{400\ \text{nm}}$ = 10,300 L cm^{-1} mol^{-1}.Yield of complex **1b** was 87.3%, red solid. Observed value in mass spectrum (FAB, *m/z*) was 735, matched well with calc. Exact mass $C_{44}H_{56}CoN_2O_4$ 735.88. Anal. Calc. (found) for $C_{44}H_{56}CoN_2O_4$: N 3.81 (3.51), C 71.82 (66.76), H 7.67 (7.12) %. The maximum absorption wavelength and molar absorption coefficient $\varepsilon_{305\ \text{nm}}$ = 25,400 L cm^{-1} mol^{-1}, $\varepsilon_{403\ \text{nm}}$ = 14,300 L cm^{-1} mol^{-1}. Yield of complex **2b** was 70.0%, red-purple solid. Observed value in mass spectrum (FAB, *m/z*) was 572, matched well with calc. exact mass $C_{30}H_{28}CoN_2O_6$ 571.50. Anal. Calc. (found) for $C_{30}H_{28}CoN_2O_6$: N 4.90 (4.90), C 63.05 (62.99), H 4.94 (4.97) %. The maximum absorption wavelength and molar absorption coefficient $\varepsilon_{310\ \text{nm}}$ = 27,800 L cm^{-1} mol^{-1}, $\varepsilon_{424\ \text{nm}}$ = 19,800 L cm^{-1} mol^{-1}. Yield of complex **3b** was 73.6%, deep-red powder. Observed value in mass spectrum (FAB, *m/z*) was 683, matched well with calc. exact mass $C_{38}H_{44}CoN_2O_6$ 683.71. Anal. Calc. (found) for $C_{38}H_{44}CoN_2O_6$: N 4.10 (4.08), C 66.76 (66.03), H 6.49 (6.46) %. The maximum absorption wavelength and molar absorption coefficient $\varepsilon_{303\ \text{nm}}$ = 23400 L cm^{-1} mol^{-1}, $\varepsilon_{424\ \text{nm}}$ = 12700 L cm^{-1} mol^{-1}.

The structures of Co^{II}(FI)$_2$ were confirmed by single crystal X-ray crystallography. The information in detail was described in Supporting Information (Tables S21 to S48).

RESULTS AND DISCUSSION

Synthesis and Characterization of Cobalt(II) Phenoxy-Imine Complexes

Cobalt(II) phenoxy-imine complexes were obtained from the reactions of cobalt(II) acetate and phenoxy-imine ligands which were converted from phenoxy-aldehydes that synthesized by phenol derivatives and formaldehyde (Scheme 3).[34,35] The cobalt(II) complexes were mainly orange-yellowish powder with two major UV–vis absorption bands at the regions of 300–310 nm and 375–424 nm (Supporting Information Fig. S1) possibly corresponding to n–π* transitions of the imine groups and ligand-to-metal charge-transfer (LMCT) transition from salicylic oxygen to cobalt,[35–37] respectively. The redox potentials ($E_{1/2}$) of cobalt(II) phenoxy-imine complexes have also been measured.[35] The values were found in the range of 0.38–0.25 V with the order of **1b** > **1a** > **3b** > **2b** > **3a** > **2a** (Supporting Information Table S2). The structures of cobalt(II) phenoxy-imine complexes were characterized by X-ray crystallography. The crystals of Co^{II}(FI)$_2$ were obtained from bilayer diffusion of dichloromethane solution with cobalt(II) phenoxy-imine complexes and methanol. According to the Oak Ridge Thermal Ellipsoid Plot (ORTEP) plots (Supporting Information Fig. S3), except complex **3b**, other five complexes have a cobalt center coordinated by two phenoxy-imine ligands with a tetrahedral configuration. And the structure of complex **1b** is consistent with

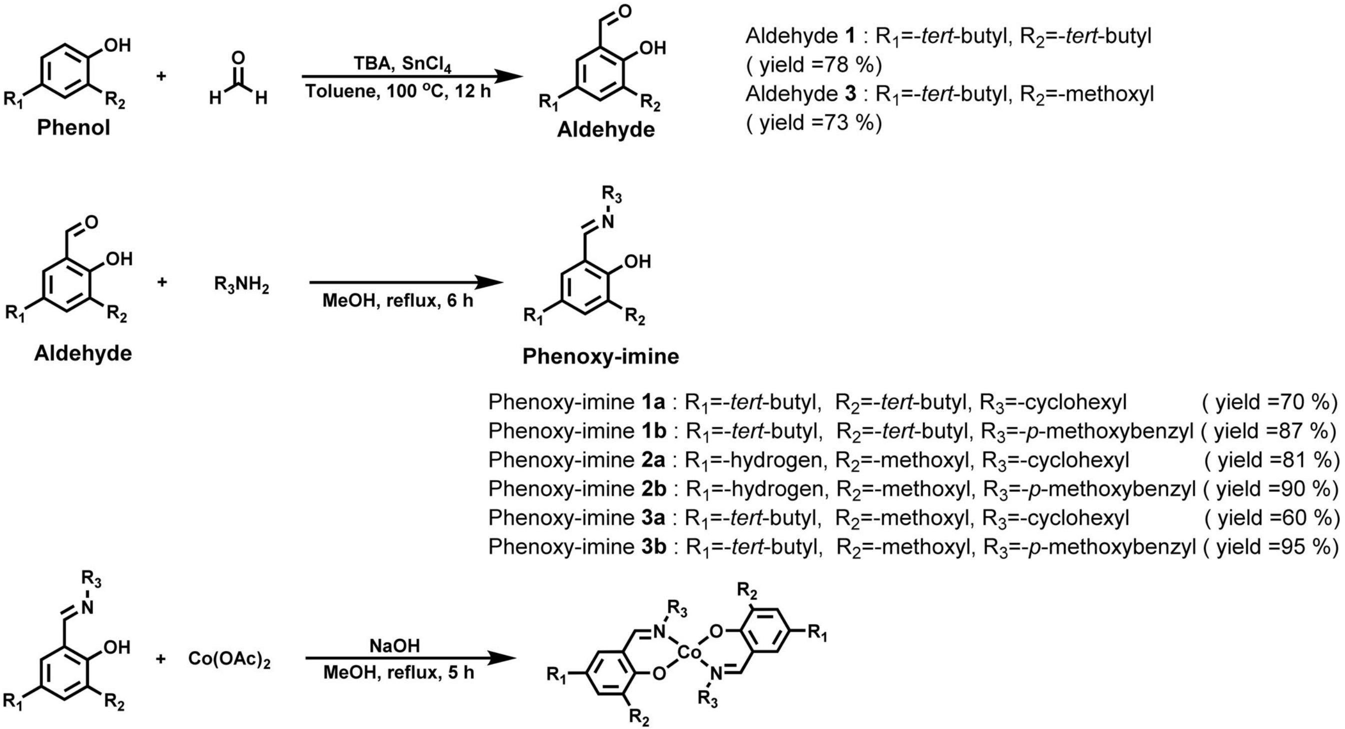

Aldehyde **1** : R_1=-*tert*-butyl, R_2=-*tert*-butyl
(yield =78 %)
Aldehyde **3** : R_1=-*tert*-butyl, R_2=-methoxyl
(yield =73 %)

Phenoxy-imine **1a** : R_1=-*tert*-butyl, R_2=-*tert*-butyl, R_3=-cyclohexyl (yield =70 %)
Phenoxy-imine **1b** : R_1=-*tert*-butyl, R_2=-*tert*-butyl, R_3=-*p*-methoxybenzyl (yield =87 %)
Phenoxy-imine **2a** : R_1=-hydrogen, R_2=-methoxyl, R_3=-cyclohexyl (yield =81 %)
Phenoxy-imine **2b** : R_1=-hydrogen, R_2=-methoxyl, R_3=-*p*-methoxybenzyl (yield =90 %)
Phenoxy-imine **3a** : R_1=-*tert*-butyl, R_2=-methoxyl, R_3=-cyclohexyl (yield =60 %)
Phenoxy-imine **3b** : R_1=-*tert*-butyl, R_2=-methoxyl, R_3=-*p*-methoxybenzyl (yield =95 %)

Complex **1a** : R_1=-*tert*-butyl, R_2=-*tert*-butyl, R_3=-cyclohexyl (yield =88 %)
Complex **1b** : R_1=-*tert*-butyl, R_2=-*tert*-butyl, R_3=-*p*-methoxybenzyl (yield =70 %)
Complex **2a** : R_1=-hydrogen, R_2=-methoxyl, R_3=-cyclohexyl (yield =63 %)
Complex **2b** : R_1=-hydrogen, R_2=-methoxyl, R_3=-*p*-methoxybenzyl (yield =78 %)
Complex **3a** : R_1=-*tert*-butyl, R_2=-methoxyl, R_3=-cyclohexyl (yield =84 %)
Complex **3b** : R_1=-*tert*-butyl, R_2=-methoxyl, R_3=-*p*-methoxybenzyl (yield =83 %)

SCHEME 3 Synthetic process with the yield of cobalt phenoxy-imine complexes.

published result.[38] The bond lengths of Co—N and Co—O are both quite similar in all five complexes as 1.99–2.00 Å and 1.89–1.91 Å, respectively. Although complex **3b** showed an octahedral configuration with the coordination of three phenoxy-imine ligands in X-ray crystallography, the mass spectrum showed the largest m/z signal at 683 (molecular weight of one cobalt and two ligands, Supporting Information Fig. S9), indicating that the complex **3b** should be more favorable to two ligands coordinated configuration during radical polymerization, similar with other five complexes. The summary of crystallographic data is shown in the Supporting Information Table S3, and the complete results of X-ray crystallography and mass spectra of cobalt(II) phenoxy-imine complexes are described in the Supporting Information. The spin state of $Co^{II}(FI)_2$ was recognized by the measurements of electron paramagnetic resonance (EPR) and superconducting quantum interference device (SQUID) using complex **1a** as the representative complex. The EPR spectrum of complex **1a** was recorded under the condition of 77 K in toluene to give a g value as 2.0010 (Supporting Information Fig. S10a). The eight peaks observed in the spectrum matched the hyperfine coupling of cobalt(II) complex. The effective magnetic moment (μ_{eff}) of complex **1a** in the solid state was measured by a SQUID magnetometer as a relatively constant value of 4.21 μ_{B} from 50 to 300 K (Supporting Information Fig. S10b), indicating a spin-only tetrahedral cobalt(II) complex.[39,40] The high-spin electron configuration of complex **1a** was demonstrated by $S = 3/2$ calculated from $\mu\mathrm{eff} = g\sqrt{S(S+1)}$ associated with $g = 2.0010$ and $\mu_{\mathrm{eff}} = 4.21$.

Polymerization of VAc Mediated by Cobalt(II) Phenoxy-Imine Complexes: Features of Controlled/Living Radical Polymerization

The polymerization of VAc was mediated by cobalt(II) phenoxy-imine complexes under the condition of $[Co^{II}]_0/[AIBN]_0/[VAc]_0 = 1/10/700$ in bulk at 60 °C and the results are shown in Table 1. Induction periods in the range of 15–60 min followed by the linearly increased first-order kinetic plots were observed [Fig. 1(a)]. During the induction period, cobalt(II) species were converted to organo-cobalt(III) complexes through the reaction with radicals.[41,42] The first-order kinetic plots implied that the radical concentration was constant,[43,44] which is the feature of cobalt-mediated controlled/living radical polymerization. However, the plots of molecular weight and polydispersity index (PDI = $M_{\mathrm{w}}/M_{\mathrm{n}}$) versus monomer conversion [Fig. 1(b)] showed that only polymerizations mediated by complexes **1a** and **3a** demonstrated the molecular weight increased properly with conversion,

TABLE 1 Polymerization of VAc Mediated by $Co^{II}(FI)_2$ in Bulk at 60 °C with the Condition of $[Co^{II}]_0/[AIBN]_0/[VAc]_0$ = 1/10/700, $[AIBN]_0$ = 0.155 M

Mediator	Time (min)	Conv.[a] (%)	$M_{n,exp}$[b] (10^3 g/mol)	$M_{n,th}$[c] (10^3 g/mol)	PDI
1a	25	3.1	92.8	1.8	1.25
	30	8.3	115.0	4.8	1.24
	35	18.4	135.0	10.8	1.27
2a	105	26.3	54.3	15.8	1.55
	120	29.8	54.3	18.0	1.55
	150	37.4	53.7	225	1.57
3a	80	24.7	84.9	14.9	1.70
	100	28.0	85.5	16.9	1.72
	120	32.4	88.0	19.6	1.70
1b	240	38.5	61.4	23.5	1.54
	300	42.6	67.5	25.9	1.52
	360	44.4	71.1	26.5	1.47
2b	360	14.5	17.0	8.7	1.86
	420	21.3	18.1	12.8	1.84
	480	23.7	18.6	14.3	1.83
3b	360	20.9	37.5	12.7	1.74
	420	27.8	38.1	16.9	1.75
	480	30.2	33.4	18.1	1.70

[a] Conversion was detected by ^{1}H NMR.

[b] M_n was determined by GPC with polystyrene as standard.

[c] $M_{n,th} = M_{w(mediator)} + M_{w(VAc)} \times 700 \times \text{Conv.}$

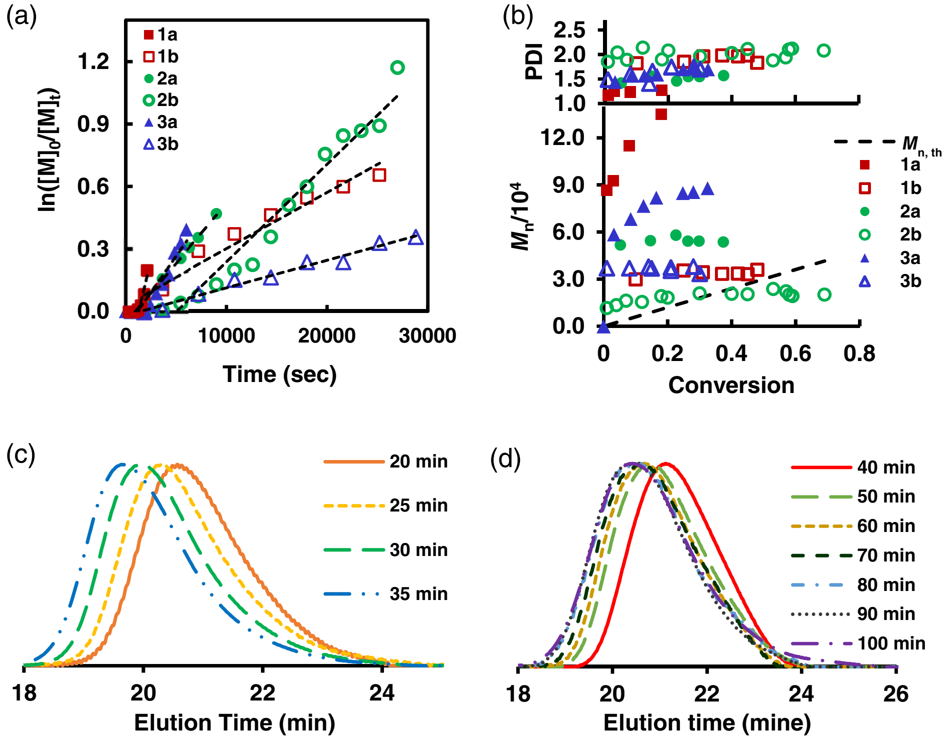

FIGURE 1 VAc polymerization mediated by $Co^{II}(FI)_2$ at 60 °C in bulk under the condition of $[Co^{II}]_0/[AIBN]_0/[VAc]_0$ = 1/10/700 with $[AIBN]_0$ = 0.155 M. (a) First-order kinetic plots. The slopes in the kinetic plots are 2.06×10^{-4} (■ complex **1a**), 2.07×10^{-5} (□ complex **1b**), 5.70×10^{-5} (● complex **2a**), 4.70×10^{-5} (○ complex **2b**), 9.65×10^{-5} (▲ complex **3a**), and 1.33×10^{-5} (△ complex **3b**). (b) The plots of M_n and PDI versus conversion. The GPC traces of VAc polymerization mediated by (c) complex **1a** and (d) complex **3a**. [Color figure can be viewed at wileyonlinelibrary.com]

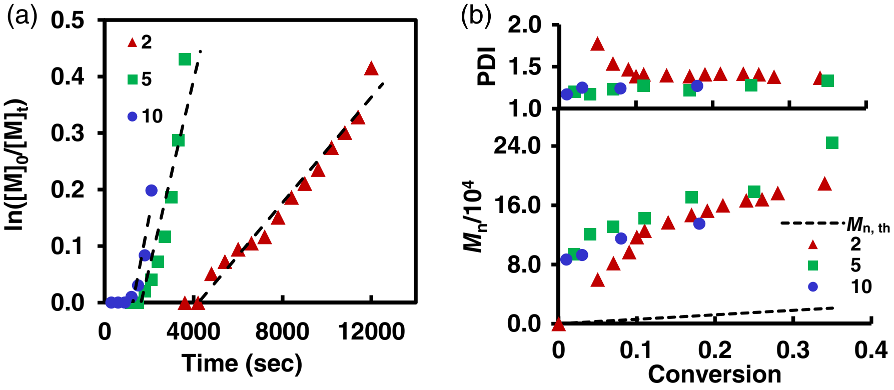

FIGURE 2 VAc polymerization mediated by complex **1a** at 60 °C under the condition of $[\mathbf{1a}]_0/[\mathrm{AIBN}]_0/[\mathrm{VAc}]_0$ = 1/X/700. (▲) X = 2, (■) X = 5, and (●) X = 10. (a) First-order kinetic plots. The slopes in kinetic plot are (▲) 4.67×10^{-5}, (■) 1.66×10^{-4}, and (●) 2.06×10^{-4}. (b) The plots of M_n and PDI versus conversion. [Color figure can be viewed at wileyonlinelibrary.com]

while the molecular weights of polymers in other polymerizations stayed constant. Comparing the shift of GPC traces of VAc polymerization mediated by complexes **1a** and **3a** [Fig. 1 (c,d)], complex **1a** was proposed to be the best mediator for C/LRP of VAc among all investigated cobalt complexes. However, the significant molecular weight deviation from theoretical value motivated us to further optimize the reaction condition and study the mechanism.

The effect of AIBN concentration in VAc polymerization mediated by complex **1a** was first evaluated. Decreasing the equivalent of AIBN, which lowered the radical concentration, caused only the longer induction period and slower polymerization rate observed by the first-order kinetic plots [Fig. 2(a)] but did not lower the PDI value nor improved the molecular weight deviation [Fig. 2(b)]. However, the slower polymerization allowed us to observe two periods of propagation in the plots of M_n and PDI versus conversion. With two equivalent of AIBN, the first period of propagation showed a faster chain growth and decline of PDI before 10% monomer conversion. Then the values of M_n and PDI obtain during the second period became similar to those in polymerization with 5 and 10 equivalent of AIBN. These two periods of propagation should be attributed to the increase of effective amount of cobalt mediators because the k_p×[radical] was relatively constant before and after 10% conversion as demonstrated by the first order kinetic plots. Since the change of AIBN did not significantly affect the molecular weight and polydispersity of the poly(vinyl acetate), indicating that the concentration of $(\mathrm{FI}^{1a})_2\mathrm{Co}^{\mathrm{III}}$-PVAc is independent to the equivalent of radical and thus the polymerization was not controlled by $\mathrm{Co}^{\mathrm{II}}/\mathrm{Co}^{\mathrm{III}}$ equilibrium. Therefore, complex **1a** was proposed to mediate the VAc polymerization via the mechanism of degenerative transfer (DT).[29]

In addition to the concentration of AIBN, VAc polymerization mediated by complex **1a** was performed under 60, 50, and 40 °C, respectively, to evaluate the temperature effect. The longer induction period and slower polymerization rate resulted from the lower radical concentration due to the slower dissociation of AIBN at declined temperature [Fig. 3(a)]. More importantly, the molecular weight deviation decreased significantly with declined temperature [Fig. 3(b)], which encouraged us to perform the polymerization at even lower temperature. However, due to the low dissociation rate of AIBN at the desired temperature, photo-initiator of TPO was selected for following polymerization. VAc polymerization was then initiated by 365 nm UV irradiation from four light bulbs (8 W for each) under the condition of $[\mathbf{1a}]_0/[\mathrm{TPO}]_0/[\mathrm{VAc}]_0$ = 1/0.8/500 at 37, 24, and 0 °C in bulk. As expected, the temperature effect to the length of induction period was similar with the polymerization initiated by AIBN [Fig. 4(a)] and the molecular weight deviation kept decreasing with lowered temperature [Fig. 4(b)]. However, because the molecular weight deviations observed in VAc polymerization at 24 and 0 °C were similar, the polymerization at 24 °C was chosen as the optimized condition due to the consideration of polymerization rate. With the adjustment of TPO equivalent, the VAc polymerization mediated by complex **1a** at 24 °C matched the features of C/LRP when the ratio of $[\mathrm{TPO}]_0/[\mathbf{1a}]_0$ equaled to 2 (Fig. 5). The monomer conversion achieved 63% in 77 min with linearly increased molecular weights that matched well with the theoretical values, relatively narrow PDIs between 1.44 and 1.75, and smoothly shifted GPC traces (Supporting Information Fig. S15b), which demonstrated that complex **1a** was a good mediator for C/LRP of VAc at room temperature. The results of VAc polymerization mediated by **1a** using different initiators and under different temperature were summarized in table 2.

High chain-end fidelity of polymer is another significant feature of C/LRP. A successful chain extension of C/LRP mediated by cobalt complex indicated that the chain-end functional group of polymer was cobalt complex. Here, macro-initiator $(\mathrm{FI}^{1a})_2\mathrm{Co}^{\mathrm{III}}$-PVAc ($M_n$ = 5.8×10^3 g/mol, PDI = 1.43) was obtained from C/LRP mediated by complex **1a** under the condition of $[\mathbf{1a}]_0/[\mathrm{TPO}]_0/[\mathrm{VAc}]_0$ = 1/5/500 at 24 °C in bulk. Then chain extension was performed by the mediation of $(\mathrm{FI}^{1a})_2\mathrm{Co}^{\mathrm{III}}$-PVAc with

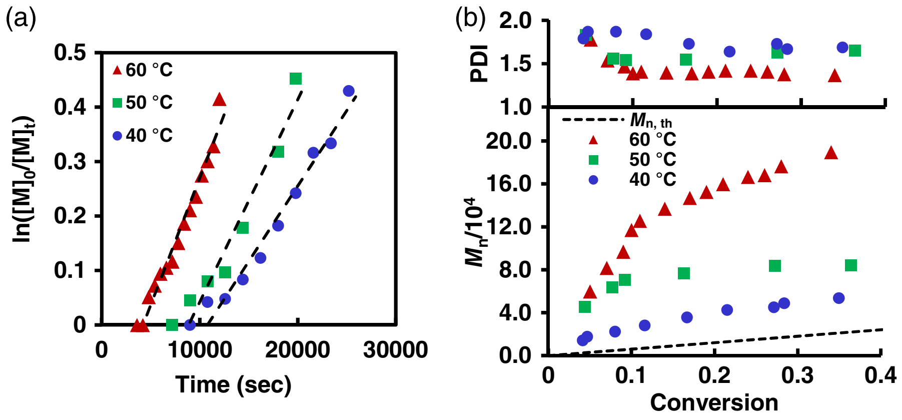

FIGURE 3 VAc polymerization mediated by complex **1a** under the condition of (▲) [**1a**]$_0$/[AIBN]$_0$/[VAc]$_0$ = 1/2/700 at 60 °C, (■) [**1a**]$_0$/[AIBN]$_0$/[VAc]$_0$ = 1/12/700 at 50 °C, and (●) [**1a**]$_0$/[AIBN]$_0$/[VAc]$_0$ = 1/70/700 at 40 °C. (a) First-order kinetic plots. The slopes in kinetic plots are (▲) 4.67×10^{-5}, (■) 3.72×10^{-5}, and (●) 2.77×10^{-5}. (b) The plots of M_n and PDI versus conversion. [Color figure can be viewed at wileyonlinelibrary.com]

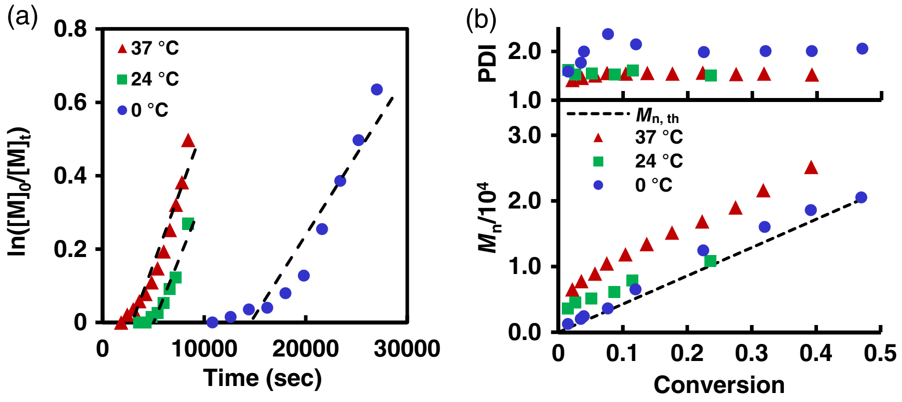

FIGURE 4 VAc polymerization mediated by complex **1a** with TPO as initiator under 365 nm irradiation with 4 bulbs of light (8 W for each) under the condition of [**1a**]$_0$/[TPO]$_0$/[VAc]$_0$ = 1/0.8/500 at (▲) 37 °C, (■) 24 °C, and (●) 0 °C. (a) First-order kinetic plots. The slopes in kinetic plots are (▲) 7.65×10^{-5}, (■) 6.92×10^{-5}, and (●) 4.38×10^{-5}. (b) The plots of M_n and PDI versus conversion. [Color figure can be viewed at wileyonlinelibrary.com]

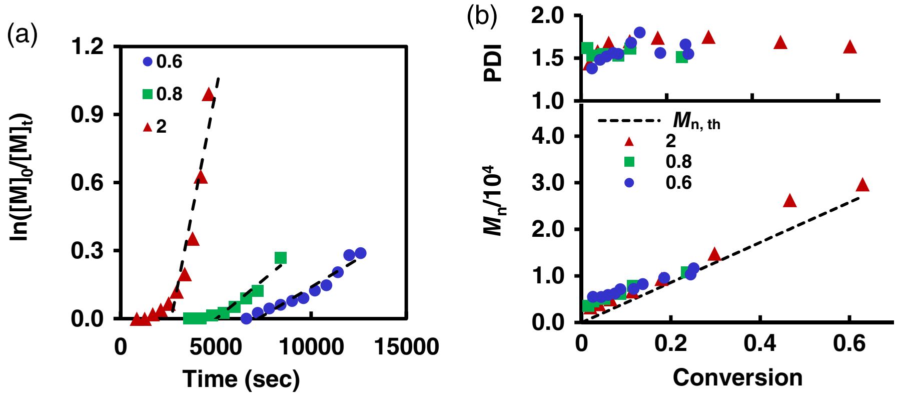

FIGURE 5 VAc polymerization mediated by complex **1a** with TPO as initiator at 24 °C under the condition [**1a**]$_0$/[TPO]$_0$/[VAc]$_0$ = 1/X/700. (▲) X = 2, (■) X = 0.8, and (●) X = 0.6. (a) First-order kinetic plots. The slopes in kinetic plots are (▲) 3.03×10^{-4}, (■) 6.92×10^{-5}, and (●) 5.02×10^{-5}. (b) The plots of M_n and PDI versus conversion. [Color figure can be viewed at wileyonlinelibrary.com]

TABLE 2 Data of VAc Polymerization Mediated by Complex **1a** in Bulk Under Different Conditions

$[1a]_0/[I]_0/[VAc]_0$	Temp. (°C)	Initiator (I)	Time (min)	Conv.[a] (%)	$M_{n,exp}$[b] (10^3 g/mol)	$M_{n,th}$[c] (10^3 g/mol)	PDI[b]
1/2/700	60	AIBN	200	34	189.6	20.5	1.37
1/5/700	60	AIBN	60	35	244.3	21.1	1.33
1/10/700	60	AIBN	35	18	135.0	10.8	1.27
1/12/700	50	AIBN	330	36	84.3	21.9	1.65
1/70/700	40	AIBN	420	35	53.7	21.1	1.69
1/0.8/500	37	TPO[d]	140	39	25.2	16.9	1.53
1/0.8/500	24	TPO[d]	140	24	10.8	10.1	1.51
1/0.8/500	0	TPO[d]	450	47	20.5	20.2	2.06
1/2/500	24	TPO[d]	77	63	29.7	27.1	1.64
1/0.6/500	24	TPO[d]	210	25	11.7	10.8	1.55

[a] Conversion was detected by ^{1}H NMR.
[b] M_n was determined by GPC with polystyrene as standard.
[c] $M_{n,th} = M_{w(mediator)} + M_{w(VAc)} \times ([VAc]_0/[Co^{II}]_0) \times$ conv.
[d] With TPO as an initiator under 365 nm irradiation with four bulbs of light (8 W for each).

the ratio of $[Co^{III}]_0/[VAc]_0 = 1/700$, generating polymer with molecular weight increased from 5.8×10^3 to 8.1×10^4 g/mol (Fig. 6). Symmetrically monomodal GPC trace was smoothly shifted to higher molecular weight, which demonstrated the chain-end functional group of polymer was cobalt phenoxy-imine complex (Table 2).

Polymerization of VAc Mediated by Cobalt(II) Phenoxy-Imine Complexes: Characterization of Catalytic Chain Transfer Polymerization

The molecular weight of poly(vinyl acetate) stayed at a relatively low and constant value during the polymerization mediated by complexes **2a**, **1b**, **2b**, and **3b**, which matched the feature of CCTP.[12] CCTP is generally used to prepare the polymers with low-molecular weight and chain end double bond. The correlation between the degree of polymerization (DP_n) and concentration of chain transfer agent ([Co]) was described by Mayo equation (eq 1),[45,46] in which the DP_0 is the degree of polymerization without chain transfer agent, [M] is the concentration of monomer, and C_s is the chain transfer constant that is corresponding to the efficiency of chain transfer agent.

$$\frac{1}{DP_n} = \frac{1}{DP_0} + C_S\left(\frac{[Co]}{[M]}\right) \qquad (1)$$

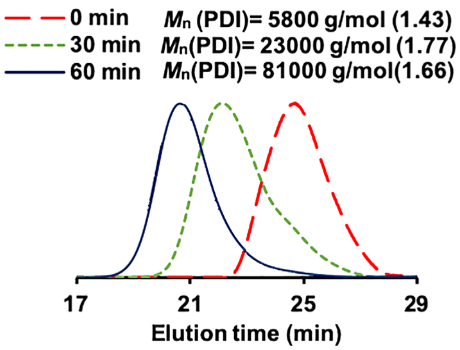

FIGURE 6 The GPC traces of $(Fl^{1a})_2Co^{III}$-PVAc and the chain extended PVAc synthesized via the mediation of $(Fl^{1a})_2Co^{III}$-PVAc at 24 °C in bulk, $[Co^{III}]_0/[VAc]_0$ = 1/700. [Color figure can be viewed at wileyonlinelibrary.com]

The values of C_s for complexes **2a**, **1b**, **2b**, and **3b** were obtained from the slope of Mayo plots with the VAc polymerization performed under the condition of $[Co^{II}]_0/[AIBN]_0/[VAc]_0 = x/100/7000$ at 60 °C in bulk (Fig. 7 and Table 3). The polymerization was stopped at monomer conversion below 15% to avoid the interferences from increased viscosity or other side reactions. Given by the slope in Mayo plots, complex **2b** showed the highest C_s as 5.41, followed by complexes **3b**, **1b**, and then **2a** (Table 3). This order matched well with the trend that complex with more electron donating and less steric hindered environment would have higher activity in CCTP.

Besides the suppression of molecular weight, generation of polymer chains with chain end double bond that could be used as "macro-monomers" for the synthesis of macromolecules with varied structures[12] is another important feature of CCTP. Thus, the poly(vinyl acetate) obtained from CCTP mediated by complex **2b**, which showed the highest C_s, was used as monomer for free-radical polymerization initiated by AIBN with the condition of $[AIBN]_0$ = 0.039 M at 60 °C in benzene [Fig. 8(a)]. The GPC traces demonstrated that the PVAc can be further polymerized to form the product with multimodal GPC trace. The chain end functionality was preliminarily estimated by the area of GPC peaks as 65% and further recognized by the integration of ^{1}H NMR spectrum as 83% [Fig. 8(b)]. The ^{1}H NMR signals of terminal double bond on PVAc were confirmed by chemical shifts at 4.56, 5.54, and 6.08 ppm by using the reaction of double bond and thiophenol reported by Poli et al.[14]

To recognize the performance of complex **2b** in CCTP of VAc, the Mayo plot with complex **2b** was compared with $Co^{II}(dmgBF_2)_2(H_2O)_2$ (Fig. 9) which was patented as a highly efficient CCT agent for the polymerization of methyl methacrylate and also reported to be able to mediate the CCTP of

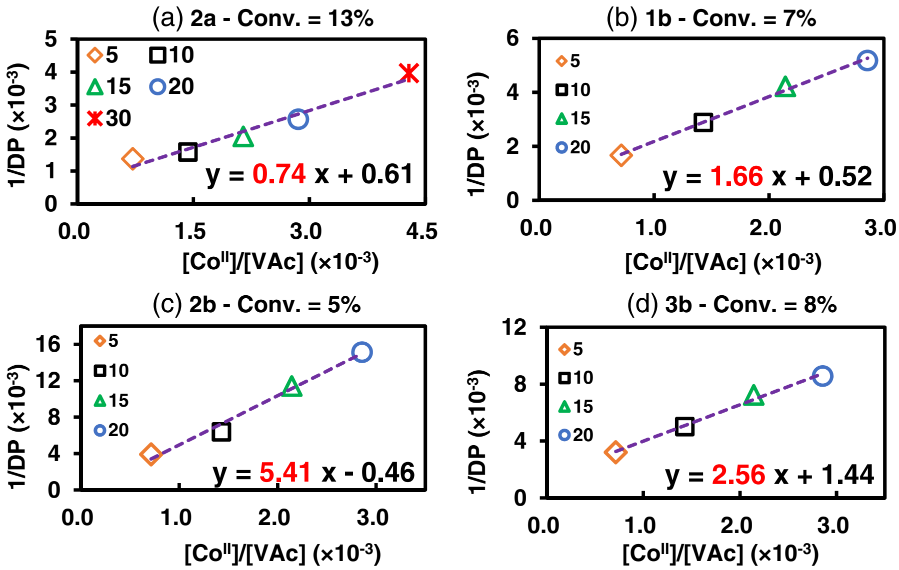

FIGURE 7 Mayo plots of VAc polymerization mediated by complexes (a) **2a**, (b) **1b**, (c) **2b**, (d) **3b** under the condition of $[Co^{II}]_0/[AIBN]_0/[VAc]_0$ = x/100/7000 at 60 °C in bulk. The monomer conversion was (a) 13%, (b) 7%, (c) 5%, (d) 8%. [Color figure can be viewed at wileyonlinelibrary.com]

TABLE 3 Chain Transfer Constant for VAc Polymerization Mediated by Different Complexes

Complex	C_s[a]
2a	0.74(07)
1b	1.66(07)
2b	5.41(47)
2b	4.70(50)[b]
3b	2.55(16)
$Co(dmgBF_2)_2(H_2O)_2$	2.23(15)

[a] In bulk.

[b] In toluene.

VAc.[15,46,47] The value of C_s for $Co^{II}(dmgBF_2)_2(H_2O)_2$ under the same condition was 2.24, which was lower than the value of 5.41 for complex **2b**, suggesting that complex **2b** was a better CCT agent than $Co^{II}(dmgBF_2)_2(H_2O)_2$ in VAc polymerization. The solvent effect has been evaluated because chain transfer to solvent is also significant in VAc polymerization[48] and thus the addition of solvent was expected to further suppress the molecular weight of polymeric product. Toluene was selected as the solvent due to a relatively high chain transfer constant in the literature.[49] Given by the Mayo plots (Fig. 10), the addition of toluene indeed further lowered the molecular weight of poly(vinyl acetate), which could be observed from either directly the value of molecular weight (from 22,000 to 11,800 g/mol when $[Co^{II}]_0/[VAc]_0$ = 10/14000 = 0.71) or the intercept of Mayo plots ($1/DP_0$) that changed from -0.46×10^{-3} to 4.38×10^{-3}. However, the slopes of Mayo plots with and without toluene were similar (5.41 and 4.70, respectively, Table 3), indicating the efficiency of chain transfer for complex **2b** was almost independent to solvent.

Polymerization of MA Mediated by Cobalt(II) Phenoxy-Imine Complexes

Cobalt(II) phenoxy-imine complexes were then investigated for C/LRP of MA under the condition of $[Co^{II}]_0/[AIBN]_0/[MA]_0$ =

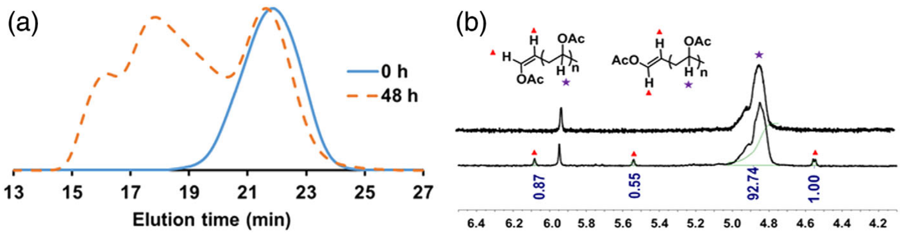

FIGURE 8 (a) The GPC traces of PVAc macro-monomer and the polymeric product of free-radical polymerization of PVAc macro-monomer at 60 °C in benzene, $[AIBN]_0$ = 0.039 M. The macro-monomer was prepared from VAc polymerization mediated by complex **2b** under the condition of $[Co^{II}]_0/[AIBN]_0/[VAc]_0$ = 1/10/700 at 60 °C in bulk. (b) ^1H NMR spectrum of PVAc macro-monomer with M_n = 6700 g/mol prepared under the condition of $[\mathbf{2b}]_0/[AIBN]_0/[VAc]_0$ = 5.5/10/700 at 60 °C in bulk before (lower) and after (upper) quenched by thiophenol. [Color figure can be viewed at wileyonlinelibrary.com]

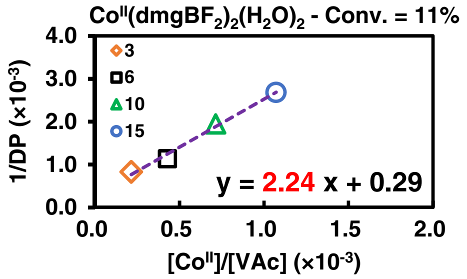

FIGURE 9 Mayo plot of VAc polymerization mediated by $Co(dmgBF_2)_2(H_2O)_2$ under the condition of $[Co^{II}]_0/[AIBN]_0/[VAc]_0$ = x/100/140,00 at 60 °C in bulk. The monomer conversion was 11%. [Color figure can be viewed at wileyonlinelibrary.com]

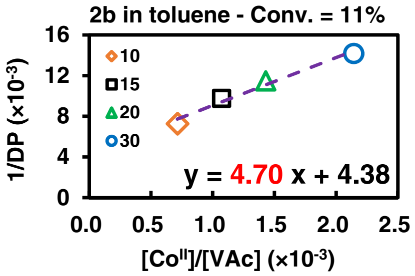

FIGURE 10 Mayo plot of VAc polymerization mediated by complex **2b** under the condition of $[Co^{II}]_0/[AIBN]_0/[VAc]_0$ = x/200/14000 at 60 °C in toluene with $[VAc]_0$ = 3.60 M. The monomer conversion was 11%. [Color figure can be viewed at wileyonlinelibrary.com]

1/1/500 in benzene 60 °C with $[MA]_0$ = 3.6 M (Supporting Information Table S20). All polymerizations showed an induction period followed by the linearly increased first-order kinetic plots [Fig. 11(a)]. However, the molecular weight of poly(methyl acrylate) approached 2.5–3.7 × 10^5 g/mol [Fig. 11(b)] at the beginning of polymerization and then stayed constant. Associated with unshifted GPC traces (Supporting Information Fig. S17) and polydispersities between 1.24 and 1.58, the cobalt(II) phenoxy-imine complexes actually could not mediate the controlled/living radical polymerization of MA.

TABLE 4 Summary of Cobalt Complexes with Varied Configuration and Chelating Atoms, as Well as the C/LRP They can Mediate

Complex	Configuration	Chelating atoms	Monomer
Co^{II}(TMP)	Square planar	N,N,N,N	VAc, MA
Co^{II}(salen*)	Square planar	N,N,O,O	VAc, MA
Co^{II}(FI)$_2$	Tetrahedral	N,N,O,O	VAc
Co^{II}(acac)$_2$	Tetrahedral	O,O,O,O	VAc

The results of VAc and MA polymerization mediated by cobalt(II) phenoxy-imine complexes and other cobalt(II) complexes are summarized in Table 4 to demonstrate the influence of coordinating atoms and configuration. All four kinds of cobalt complexes can control the polymerization of VAc but only Co^{II}(TMP) and Co^{II}(salen*), which have a square planar configuration, can mediate the C/LRP of MA. Even the Co^{II}(FI)$_2$ has the same chelating atoms with Co^{II}(salen*), still could not control the MA polymerization, suggesting that configuration and thus spin state were more critical than chelating atoms for the controlled/living radical polymerization of MA and perhaps a broader scope of vinyl monomers.

Mechanism

Cobalt(II) phenoxy-imine complexes have been demonstrated to be capable of mediating controlled/living radical polymerization and CCTP of VAc depending on the ligand structure, implying these two polymerizations are correlated and could be competing reactions. The mechanism of cobalt-mediated radical polymerization includes C/LRP and CCTP is thus proposed as Scheme 4. In most cases, both C/LRP and CCTP mediated by cobalt complexes start from the reaction of cobalt(II) complexes and radicals to form the organo-cobalt(III) species,[7,33,50]

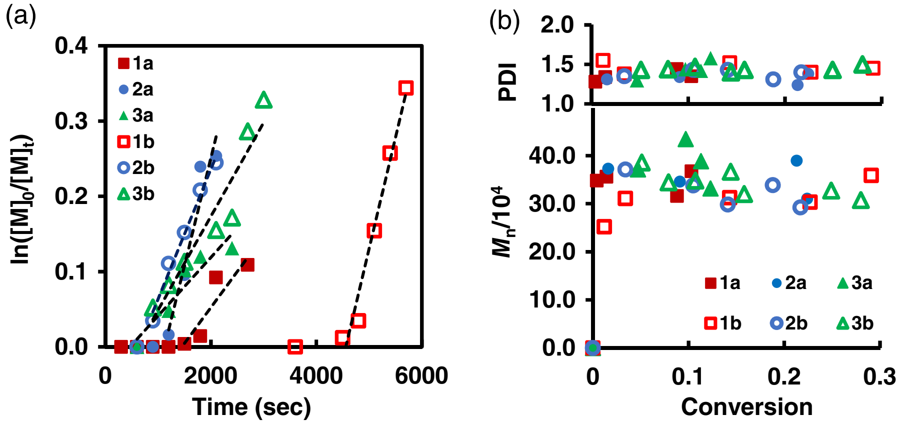

FIGURE 11 MA polymerization mediated by Co^{II}(FI)$_2$ at 60 °C in benzene under the condition of $[Co^{II}]_0/[AIBN]_0/[MA]_0$ = 1/1/500, $[MA]_0$ = 3.6 M. (a) First-order kinetic plots. The slope in kinetic plot are 1.00 × 10^{-4} (■ **1a**), 2.96 × 10^{-5} (□ **1b**), 2.86 × 10^{-4} (● **2a**), 1.72 × 10^{-4} (○ **2b**), 8.00 × 10^{-5} (▲ **3a**), and 1.24 × 10^{-4} (△ **3b**). (b) The plots of M_n and PDI versus conversion. [Color figure can be viewed at wileyonlinelibrary.com]

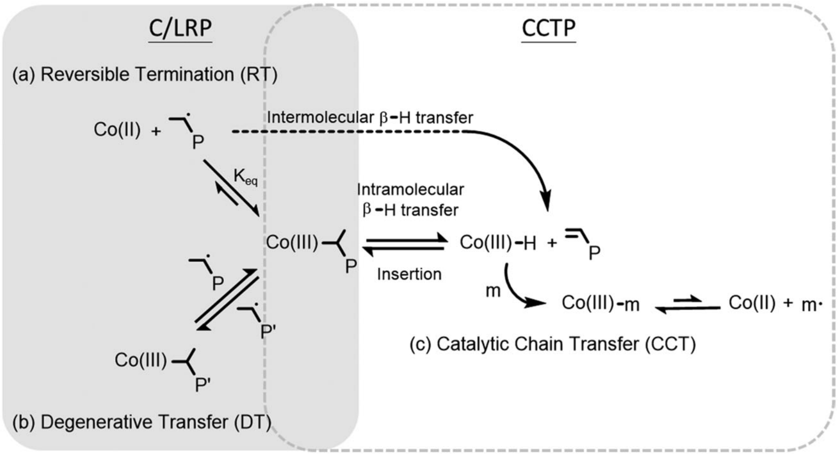

SCHEME 4 Correlation of RT, DT, and CCT mechanisms in cobalt-mediated radical polymerization.

resulting in an induction period.[17,25,30,31,40] C/LRPs directly initiated by organo-cobalt(III) species, which was synthesized from cobalt(II) complex in advance, do not have induction period.[42,51,52] If the Co—C bond dissociation energy of organo-cobalt(III) species is in a proper range that cobalt(II) complexes and radicals can be regenerated via bond homolysis to initiate the polymerization without addition of external radicals, the mechanism of C/LRP could be rationalized as reversible termination (RT) [Scheme 4(a), RT]. In this case, the radical concentration is mainly dominated by the equilibrium of cobalt(II) and organo-cobalt(III) species ($[P\bullet] = [Co(III)\text{-}P]/([Co(II)] \times K_{eq})$), which can be another characteristic to recognize RT mechanism. However, when the Co—C bond dissociation energy is too high for organo-cobalt(III) species to release the radicals, the initiation of polymerization requires an external radical source such as AIBN or TPO and the radical concentration is mainly determined by the concentration of external radical source ($[P\bullet] = (k_i[\text{initiator}]/2k_t)^{1/2}$). This mechanism is known as DT [Scheme 4(b)], in which the propagating radicals rapidly exchange with the organic radicals on organo-cobalt(III) species to provide an equal chance for each polymer chain to grow. Both RT and DT can achieve the C/LRP and are distinguished by the source and concentration of radicals.[29,30] Another pathway is known as CCT [Scheme 4(c))] in which the metal center of organo-cobalt(III) species abstracts the hydrogen from the organic group to form the cobalt hydride and the corresponding vinyl species.[7,50] Although this reaction was proposed to be an intramolecular process in our study due to the occurrence of induction period, implying that the formation of organo-cobalt(III) species is prior to the polymerization, the possibility of coexistence of β-H transfer via intermolecular reaction between cobalt(II) complex and radicals cannot be excluded.[53–55] The cobalt hydride is highly active and can react with monomers or other vinyl compounds to generate organo-cobalt(III) species. Because the long propagating radicals (P•) are replaced by small radicals (m•), and polymers with double bond chain end could be formed by β-H transfer, this process would suppress the molecular weight of polymer and generate macro-monomer for further polymerization. Therefore, it could be rationalized that the change of coordination environment of cobalt(II) phenoxy-imine complexes by modifying the ligands could shift their tendency of polymerization pathways.

CONCLUSIONS

A series of cobalt(II) phenoxy-imine complexes have been prepared and applied to mediate the radical polymerization of VAc and MA to study the influence of coordination configuration and chelating atoms to the control of radical polymerization. Complex **1a** showed the best control behavior of VAc polymerization supported by the living characters of molecular weights not only increasing linearly with conversion but also matching with the theoretical values and moderate molecular weight distributions at room temperature. Compared to the published results using Co^{II}(TMP), Co^{II}(salen*), and $Co^{II}(acac)_2$, coordination configuration is more critical to the mediation of controlled/living radical polymerization than chelating atoms, demonstrated by that cobalt complexes with square planar structure like Co^{II}(TMP) and Co^{II}(salen*) can mediate C/LRP of both unconjugated monomer of VAc and conjugated monomer of MA, but $Co^{II}(FI)_2$ and $Co^{II}(acac)_2$ can only control VAc polymerization, even Co^{II}(salen*) and $Co^{II}(FI)_2$ have the same chelating atoms. In addition to controlled/living radical polymerization, $Co^{II}(FI)_2$ also could mediate the CCTP of VAc. Complex **2b** showed the highest activity in CCTP of VAc, even higher than the famous CCT agent of $Co(dmgBF_2)_2(H_2O)_2$, supported by the larger slope in the Mayo plots. Given by the polymerization of VAc mediated by these six cobalt(II) phenoxy-imine complexes, the characteristics of controlled/living radical polymerization become more significant when the ligand has more bulky and less electron-donating substituents. Reversely, the features of CCTP would be more obvious. The different performance of cobalt(II) phenoxy-imine complexes in VAc polymerization could be rationalized by the proposed mechanism correlating the pathways of RT and DT in C/LRP and the reaction of CCT in CCTP and thus illustrates the potential of $Co^{II}(FI)_2$ in the application of combining C/LRP and CCTP techniques.

ACKNOWLEDGMENT

We thank the Ministry of Science and Technology, Taiwan, (MOST 107-2113-M-007-014) for support of this research. We also thank Chuan Huang and Shan-Cheng Tang for their help to the experiments.

REFERENCES AND NOTES

1 B. R. Smirnov, V. D. Plotnikov, B. V. Ozerkovskii, V. P. Roshchupkin, N. S. Enikolopyan, *Polym. Sci. U.S.S.R* **1981**, *23*, 2807.

2 N. S. Enikolopyan, B. R. Smirnov, G. V. Ponomarev, I. M. Belgovskii, *J. Polym. Sci. A-Polym. Chem.* **1981**, *19*, 879.

3 A. Gridnev, *J. Polym. Sci. A-Polym. Chem.* **2000**, *38*, 1753.

4 D. J. Forster, J. P. A. Heuts, F. P. Lucien, T. P. Davis, *Macromolecules* **1999**, *32*, 5514.

5 J. P. A. Heuts, D. Kukulj, D. J. Forster, T. P. Davis, *Macromolecules* **1998**, *31*, 2894.

6 K. G. Suddaby, D. R. Maloney, D. M. Haddleton, *Macromolecules* **1997**, *30*, 702.

7 J. P. A. Heuts, D. J. Forster, T. P. Davis, B. Yamada, H. Yamazoe, M. Azukizawa, *Macromolecules* **1999**, *32*, 2511.

8 S. C. J. Pierik, B. Smeets, A. M. van Herk, *Macromolecules* **2003**, *36*, 9271.

9 M. D. Haddleton, D. R. Maloney, K. G. Suddaby, *Macromolecules* **1996**, *29*, 481.

10 K. G. Suddaby, D. M. Haddleton, J. J. Hastings, S. N. Richards, J. P. O'Donnell, *Macromolecules* **1996**, *29*, 8083.

11 W. Wang, P. A. Stenson, A. Marin-Becerra, J. McMaster, M. Schröder, D. J. Irvine, D. Freeman, S. M. Howdle, *Macromolecules* **2004**, *37*, 6667.

12 A. A. Gridnev, S. D. Ittel, *Chem. Rev.* **2001**, *101*, 3611.

13 N. G. Engelis, A. Anastasaki, R. Whitfield, G. R. Jones, E. Liarou, V. Nikolaou, G. Nurumbetov, D. M. Haddleton, *Macromolecules* **2018**, *51*, 336.

14 E. V. Bellan, L. Thevenin, F. Gayet, C. Fliedel, R. Poli, *ACS Macro. Lett.* **2017**, *6*, 959.

15 J. P. A. Heuts, N. M. B. Smeets, *Polym. Chem.* **2011**, *2*, 2407.

16 S. Banerjee, E. V. Bellan, F. Gayet, A. Debuigne, C. Detrembleur, R. Poli, B. Améduri, V. Ladmiral, *Polymers* **2017**, *9*, 702.

17 A. Debuigne, J. Warnant, R. Jérôme, I. Voets, A. de Keizer, M. A. Cohen Stuart, C. Detrembleur, *Macromolecules* **2008**, *41*, 2353.

18 P. G. Falireas, V. Ladmiral, A. Debuigne, C. Detrembleur, R. Poli, B. Ameduri, *Macromolecules* **2019**, *52*, 1266.

19 C. Fliedel, R. Poli, *J. Organomet. Chem.* **2019**, *880*, 241.

20 J. Demarteau, B. Améduri, V. Ladmiral, M. A. Mees, R. Hoogenboom, A. Debuigne, C. Detrembleur, *Macromolecules* **2017**, *50*, 3750.

21 S. Yamago, B. Ray, K. Iida, J.-i. Yoshida, T. Tada, K. Yoshizawa, Y. Kwak, A. Goto, T. Fukuda, *J. Am. Chem. Soc.* **2004**, *126*, 13908.

22 A. Kermagoret, Y. Nakamura, M. Bourguignon, C. Detrembleur, C. Jérôme, S. Yamago, A. Debuigne, *ACS Macro Lett.* **2014**, *3*, 114.

23 J. J. Lessard, L. F. Garcia, C. P. Easterling, M. B. Sims, K. C. Bentz, S. Arencibia, D. A. Savin, B. S. Sumerlin, *Macromolecules* **2019**, *52*, 2105.

24 B. B. Wayland, G. Poszmik, S. L. Mukerjee, M. Fryd, *J. Am. Chem. Soc.* **1994**, *116*, 7943.

25 A. Debuigne, J. R. Caille, R. Jerome, *Angew. Chem. Int. Ed.* **2005**, *44*, 1101.

26 K. S. S. Kumar, Y. Gnanou, Y. Champouret, J.-C. Daran, R. Poli, *Chem. A Eur. J.* **2009**, *15*, 4874.

27 Y.-C. Lin, Y.-L. Hsieh, Y.-D. Lin, C.-H. Peng, *Macromolecules* **2014**, *47*, 7362.

28 Y. K. Redjel, L. Thevenin, J.-C. Daran, M. Benslimane, R. Poli, C. Fliedel, *Polyhedron* **2019**, *158*, 83.

29 Y. H. Chen, H. H. Lu, J. Q. Li, C. H. Peng, *Reversible Deactivation Radical Polymerization: Mechanisms and Synthetic Methodologies; ACS Symposium Series 1284*; American Chemical Society: Washington, DC, **2018**, p. 335.

30 C. M. Liao, C. C. Hsu, F. S. Wang, B. B. Wayland, C. H. Peng, *Polym. Chem.* **2013**, *4*, 3098.

31 C. S. Hsu, T. Y. Yang, C. H. Peng, *Polym. Chem.* **2014**, *5*, 3867.

32 Y. Zhao, M. Yu, S. Zhang, Z. Wu, Y. Liu, C.-H. Peng, X. Fu, *Chem. Sci.* **2015**, *6*, 2979.

33 Y. Zhao, S. Zhang, Z. Wu, X. Liu, X. Zhao, C.-H. Peng, X. Fu, *Macromolecules* **2015**, *48*, 5132.

34 G. W. Theaker, C. Morton, P. Scott, *Dalton Trans.* **2008**, 6883.

35 V. T. Kasumov, M. Özdemir, E. Tas, Ö. Sahin, *Transit. Met Chem.* **2005**, *30*, 191.

36 L. Sacconi, M. Ciampolini, F. Maggio, F. P. Cavasino, *J. Am. Chem. Soc.* **1962**, *84*, 3246.

37 M. A. Hitchman, *Inorg. Chem.* **1977**, *16*, 1985.

38 B. Chakraborty, S. Banerjee, *J. Coord. Chem.* **2013**, *66*, 3619.

39 B. S. Jaynes, L. H. Doerrer, L. Shuncheng, J. Stephen, *Inorg. Chem.* **1995**, *34*, 5735.

40 S. A. Carabineiro, L. C. Silva, P. T. Gomes, L. C. J. Pereira, L. F. Veiros, S. I. Pascu, M. T. Duarte, S. Namorado, R. T. Henriques, *Inorg. Chem.* **2007**, *46*, 6880.

41 C.-H. Peng, J. Scricco, S. Li, M. Fryd, B. B. Wayland, *Macromolecules* **2008**, *41*, 2368.

42 A. Debuigne, Y. Champouret, R. Jérôme, R. Poli, C. Detrembleur, *Chem. A Eur. J.* **2008**, *14*, 4046.

43 G. Moad, E. Rizzardo, D. H. Solomon, B. ALJ, *Polym. Bull.* **1992**, *29*, 647.

44 S. Li, B. d. Bruin, C.-H. Peng, M. Fryd, B. B. Wayland, *J. Am. Chem. Soc.* **2008**, *130*, 13373.

45 G. Odian, *Principles of Polymecrization*; Wiely: New York, NY, **1981**.

46 A. Rudin, *The Elements of Polymer Science and Engineering*; Academic Press: New York, NY, **1982**.

47 A. H. Janowicz, U.S. Patent, 4,694,054, 1991.

48 S. Salehpour, M. A. Dubé, *Green Chem.* **2008**, *10*, 321.

49 F. R. Mayo, *J. Am. Chem. Soc.* **1943**, *65*, 2324.

50 J. P. A. Heuts, D. J. Forster, T. P. Davis, *Macromolecules* **1999**, *32*, 3907.

51 A. Debuigne, J.-R. Caille, N. Willet, R. Jérôme, *Macromolecules* **2005**, *38*, 9488.

52 M. Hurtgen, A. Debuigne, C. Jérôme, C. Detrembleur, *Macromolecules* **2010**, *43*, 886.

53 S. Slavin, K. McEwan, D. M. Haddleton, In *Polymer Science*; A. Comprehensive Reference, K. Matyjaszewski, M. Möller, Eds.; Elsevier BV: Amsterdam, **2012**; Vol. *3*, p. 249.

54 A. Debuigne, R. Poli, C. Jérôme, R. Jérôme, C. Detrembleur, *Prog. Polym. Sci.* **2009**, *34*, 211.

55 G. E. Roberts, C. Barner-Kowollik, T. P. Davis, J. P. A. Heuts, *Macromolecules* **2003**, *36*, 1054.